13

Calculation of electric field strength sensor in photonic integrated circuit configuration with polarisation splitter

© I.V. Kuznetsov[1], A.S. Perin[1,2], A.A. Zhuravlev[3]

[1] Tomsk State University of Control Systems and Radioelectronics,
Tomsk, Russia
[2] V.E. Zuev Institute of Atmospheric Optics, Siberian Branch of the Russian Academy of Sciences,
Tomsk, Russia
[3] Perm Scientific and Production Instrument-Making Company,
Perm, Russia
e-mail: igor.v.kuznetsov@tusur.ru

Received May 03, 2024
Revised September 24, 2024
Accepted October 30, 2024

A model of an electric field strength sensor consisting of a Pockels cell, a polarisation splitter and a Mach-Zehnder interferometer in one of the arms has been considered. The results of calculating the dependence of the normalised intensity of optical radiation on the magnitude of the externally applied electric field strength are presented. The extinction coefficient was -1.5 dB, the upper limit of measurement was 500 V/m at the half-length of the dipole antenna 2 mm, the bandwidth was 10 GHz.

Keywords: lithium niobate, Pockels cell, polarisation splitter, photonic integrated circuit.

DOI: 10.61011/EOS.2024.11.60316.6493-24

Measurement of the electric field strength is a pressing problem facing science and industry. Solving this problem is especially critical for radio-electronic industry because, according to modern requirements, all radio-electronic products must be certified for electromagnetic compatibility.

The most common class of devices for measuring electric field strength in the commercial sector are diode-based electric field probes.

An alternative to diode-based electric field probes are sensors using optical radiation as a carrier. Electric field strength detection in such devices is carried out due to modulation of optical radiation by electro-optical effects [3–5].

One of the possible ways to implement an electro-optical electric field strength sensor is a configuration based on a Mach-Zehnder interferometer (MZI) [6,7]. This device consists of two Y-couplers connected by straight waveguides called „arms". One of the arms is usually surrounded by an antenna or an array of antennas (dipole or patch antennas are more commonly used). The size of the antenna elements is on the order of units of millimetres, forcing millimetre distances between the interferometer's arms. If the optical scheme is implemented based on waveguides formed by titanium diffusion into a bulk lithium niobate crystal ($LiNbO_3$) [6,7], this is not a significant limitation because the low optical contrast of such waveguides, in its turn, makes it necessary to provide large bending radii in the Y-coupler in the course of design. This is not the case for a photonic integrated circuit based on a $LiNbO_3$ thin film on a silicon oxide insulator (SiO_2), because the high optical contrast allows significantly reducing the geometrical dimensions of the optical circuit compared to the implementation on a bulk crystal.

This paper will consider an alternative optical scheme comprising a Pockels cell (PC), a polarisation splitter (PS) and a MZI with a polarisation converter in one arm [8,9]. By using the PC as the sensing element, the antenna size constraints will be avoided.

Thus, the purpose of the work is to calculate an electric field strength sensor in an PC configuration with an integrated PS in a MZI with a polarisation converter in the form of a photonic integrated circuit. In this paper we will calculate the power transfer coefficients of optical radiation propagation through such a structure taking into account the externally applied electric field.

The device under consideration is a Pockels cell based on a thin film of a lithium niobate crystal ($LiNbO_3$) on a SiO_2 insulator, docked to a polarisation splitter in the form of a directional splitter with zero gap [10,11], to the output of which the MZI is docked with the polarisation converter. The device diagram is shown in Fig. 1, the coordinate axes in the figure denote the orientation of the $LiNbO_3$. The waveguide cladding is made of SiO_2.

Table 1 shows the circuit parameters shown in Fig. 1, Table 2 — physical parameters of the model [11].

Linearly polarised optical radiation with an angle φ_0 of inclination to the axis Z of a thin $LiNbO_3$crystalline film is injected into the Pockels cell (section (a) in Fig. 1). As a result of the birefringence, the linear polarisation of the optical radiation is converted into an elliptical polarisation. Additionally, the effect of an electric field applied along the axis Z of the film causes a change in the magnitude of

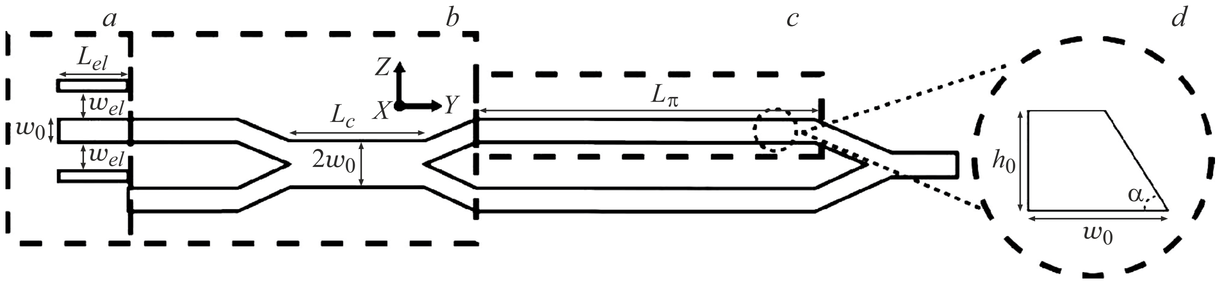

Figure 1. Schematic diagram of the device under consideration: (*a*) PC, (*b*) PS, (*c*) polarisation converter, (*d*) cross section of the polarisation converter waveguide core.

Table 1. Geometrical parameters of the model

Parameter	Parameter, unit	Value
w_0	Width of the waveguide core, nm	600
h_0	Height of the waveguide core, nm	300
w_{el}	Gap between the waveguide and the electrode, μm	1
L_{el}	Length of the electrodes, mm	5
L_c	Length of the two-mode interference zone, μm	20.65
L_π	Length of the polarisation converter, μm	21.13
α	Rake angle of the polarisation converter wall, deg	70

the extraordinary refractive index and therefore a change in the phase overlap between the components corresponding to the ordinary and extraordinary polarisation states. As noted above, real devices use antennas [6,7] to transmit the external electric field to waveguide structures. In this paper, instead of antennas, strip electrodes will be used in the calculation, since the development of the receiving antenna is beyond the scope of this paper. Also note that in practical implementation, the electrodes can be used for the task of the operating point position of the device by applying a bias voltage. In this study, the Pockels effect was calculated only directly along the axis Z of the thin film, since the electrodes associated with the antennas apply the field along this direction. Consequently, in other directions, the electric field will not be enhanced and will be small compared to the field applied along the Z axis.

The operation concept of the used PS is based on the two-mode interference arising in the wide part of the PS between the fundamental mode and the first-order mode. The width of the interference zone is selected to ensure the two-mode regime, and the length of this zone is chosen to be sufficient to ensure separation of the orthogonally polarised components in space. The methodology for selecting the geometrical parameters to achieve polarisation separation is described in detail in [6,7]. The finite element method in the frequency domain was used to calculate the geometry by calculating the propagation of optical radiation. The transmission coefficient for the TE-mode was about 40%, and for the TM-mode 71.3%. The losses in the PS are explained by the presence of radiation scattering into the waveguide cladding.

The scheme uses a polarisation converter based on a waveguide with a bevelled wall [8,9]. The operating principle of the polarisation converter used is the hybridisation of the fundamental TE- and TM-modes propagating in the waveguide, achieved by breaking the symmetry of the waveguide core by bevelling one of its walls. The optimum length of the converter to ensure 100% conversion from TE to TM can be obtained by the formula:

$$L_\pi = \frac{\pi}{\beta_1 - \beta_2}, \quad (1)$$

where β_1, β_2 — propagation constants of the fundamental TE- and TM-modes. For the parameters described in Tables 1 and 2, the propagation constants were: $\beta_1 \approx 6.22 \cdot 10^6$, $\beta_2 \approx 6.06 \cdot 10^6$ rad/m, respectively, thus $L_\pi = 21.13\,\mu$m.

The magnitude of the optical intensity at the MZI output depends on the phase difference $\Delta\varphi$ between the waves propagating along different legs and is determined from the formula:

$$I = \frac{1}{2} I_0 \cdot (1 - \cos\Delta\varphi) \quad (2)$$

where I_0 — input intensity. Value $\Delta\varphi$ can be decomposed into a constant component $\Delta\varphi_c$, determined by the waveguide structure, and a component $\Delta\varphi_f$ dependent on

Table 2. Physical parameters of the model

Parameter	Parameter , Unit	Value
n_0	Cladding refractive index (SiO_2)	1.44 [12]
n_1	Ordinary refractive index	2.2111 [13]
n_2	Extraordinary refractive index	2.1376 [13]
λ	Radiation wavelength, nm	1550
ε_0	Relative permittivity of the cladding (SiO_2)	4 [14]
ε_{11}	Components of the relative permittivity tensor	84 [15]
ε_{33}	$LiNbO_3$	30 [15]
r_{13}	Components of the electro-optical coefficient tensor $LiNbO_3$	8.6 [15]
r_{22}		3.4 [15]
r_{33}		30.8 [15]
r_{51}		28 [15]
φ_0	Angle of inclination of the polarisation plane to the optical axis of the crystal, deg	45

the magnitude of the electric field applied to the PC. Let us express both components through the formula:

$$\Delta\varphi_c = \frac{2\pi}{\lambda}(n_1 - n_2)L, \tag{3}$$

where $L \approx 5060\,\mu$m — the length of the optical circuit. From (3), we find that the constant phase difference due to device geometry is 480.011π or $2.036°$ modulo $360°$.

To determine the non-constant phase offset component, we can use the formula:

$$\Delta\varphi_f = -\frac{\pi \cdot n_2^3 \cdot r_{33}\left(E + \frac{U_B}{w_0 + 2w_{el}}\right) \cdot L}{\lambda} \tag{4}$$

where E — externally applied electric field, U_B — bias voltage. Fig. 2 shows the dependence of relative intensity at the MZI output on the value of the applied electric field, obtained by calculating the propagation of optical radiation through the circuit (Fig. 1) taking into account the electric field applied to the electrodes.

As can be seen from Fig. 2, the half-wave intensity of the above configuration is of the order of 1 MV/m, which, taking into account that the distance between the electrodes is of the order of $2.3\,\mu$m is equivalent to a voltage of 2 V applied to the electrodes. If instead of the electrodes a dipole antenna with a half-length dipole $L_d = 2$ mm is installed, then, taking into account the gain of such an antenna, which can be found by the formula [9]:

$$F = \frac{L_d}{w_{el}} = \frac{2\,\text{mm}}{10\,\mu\text{m}} = 2000, \tag{5}$$

the upper limit of intensity measurement will be 500 V/m. The small extinction coefficient (-1.5 dB) is due to the large difference between the transmission coefficients of the PS.

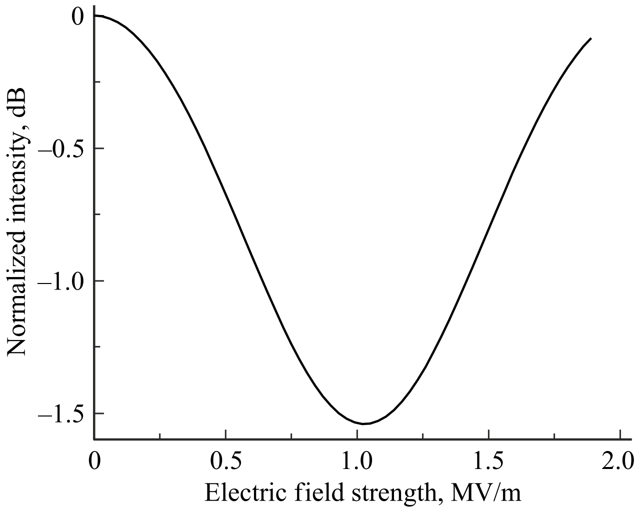

Figure 2. Dependence of the relative intensity at the MZI output on the value of the applied electric field.

Let's estimate the frequency range of the sensor by using the formula linking the electrode bandwidth -3 dB with its length:

$$\Delta f_{-3\text{dB}} = \frac{1.4c}{\pi\left|n_e - \sqrt{\frac{\varepsilon_r}{2}}\right|L_{el}} \tag{6}$$

where $c = 3 \cdot 10^8$ m/s — the speed of light in vacuum, $\varepsilon_r = 44$ — the relative dielectric constant of $LiNbO_3$ [16]. Hence:

$$\Delta f_{-3\text{dB}} = \frac{1.4 \cdot 3 \cdot 10^8}{\pi \cdot \left|2.137 - \sqrt{\frac{44+1}{2}}\right| \cdot 5 \cdot 10^{-3}} = 10.26\,\text{GHz}$$

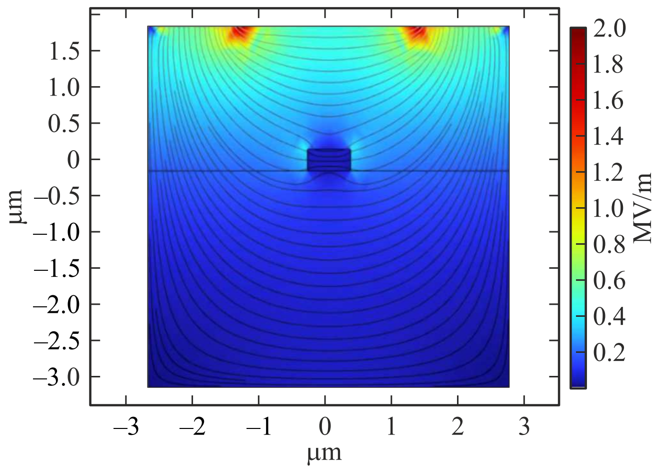

Figure 3. The electric field distribution in the cross-section of the PC at an applied voltage of 2 V.

Fig. 3 shows the electric field distribution in the cross section of the PC at an applied voltage of 2 V and a cladding height of 2 μm.

Fig. 3 shows that due to the large difference in dielectric constants between $LiNbO_3$ and SiO_2 refraction of the field lines in the region of the waveguide core and reflection of the electric field from its walls are observed. The large magnitude of electric field reflections reduces the efficiency of the electro-optic effect and can be minimised by using alternative buffer materials with higher dielectric constant, such as $LaAlSiInO_x$ [17].

Thus, an alternative optical scheme for an electro-optic electric field strength sensor including a Pockels cell, a polarisation splitter and an MZI with a polarisation converter in one of the arms was calculated. The extinction coefficient was -1.5 dB, the upper measurement limit was 500 V/m (at a half-length of the dipole antenna of 2 mm), and the bandwidth was 10 GHz.

Funding

The study was carried out under the state order of the Ministry of Science and Higher Education of the Russian Federation (subject № FEWM-2022-0004 „Research and development of manufacturing methods for integrated optical waveguides and elements based on them") in terms of problem statement and simulation, as well as under the state order of Institute of Atmospheric Optics of the Siberian Branch of the RAS regarding calculations.

Conflict of interest

The authors declare that they have no conflict of interest.

References

[1] H. Bassen, G. Smith, in *IEEE Transactions on Antennas and propagation* (IEEE, 1983), vol. 31, p. 710. DOI: 10.1109/TAP.1983.1143126
[2] Y. Yan, Y. Hu, L. Wang, X. Qiuan, W. Zhang, K. Reda, J. Wu, G. Zhang, Measurement, **169**, 108506 (2021). DOI: 10.1016/j.measurement.2020.108506
[3] J. Peng, S. Jia, J. Bian, S. Zhang, J. Liu, X. Zhou. Sensors, **19** (13), 2860 (2019). DOI: 10.3390/s19132860
[4] H. Jung. Fiber and Integrated Optics, **35** (4), 161 (2016). DOI: 10.1080/01468030.2016.1198508
[5] G.D. Boyd, Robert C. Miller, K. Nassau, W.L. Bond, A. Savage. Appl. Phys. Lett., **5** (11), 234 (1964). DOI: 10.1063/1.1723604
[6] J. Zhang, Z. Zhao, C. Li, Y. Li. Fiber and Integrated Optics, **36** (4–5), 157 (2017). DOI: 10.1080/01468030.2017.1357770
[7] J. Zhang, F. Chen, B. Liu. IEEE Microwave and Wireless Components Lett., **30** (10), 1009 (2020). DOI: 10.1109/LMWC.2020.3019448
[8] V.P. Tzolov, M. Fontaine. Opt. Commun., **127** (1–3), 7 (1996). DOI: 10.1016/0030-4018(96)00039-9
[9] Z. Huan, R. Scarmozzino, G. Nagy, J. Steel, R.M. Osgood. IEEE Photonics Technology Lett., **12** (3), 317 (2000). DOI: 10.1109/68.826926
[10] R. Sattibabu, P. Kunar Dey, B.N. Shivakiran Bhaktha, P. Ganguly. Results in Optics, **8**, 100262 (2022). DOI: 10.1016/j.rio.2022.100262
[11] I.V. Kuznetsov, A.S. Perin. Opt. i spektr., **131** (11), 1529 (2023) (in Russian).
[12] I.H. Malitson. JOSA, **55** (10), 1205 (1965). DOI: 10.1364/JOSA.55.001205
[13] D.E. Zelmon, D.L. Small, D. Jundt. JOSA B., **14** (12), 3319 (1997). DOI: 10.1364/JOSAB.14.003319
[14] S. Holten; H. Kliem. J. Appl. Phys., **93** (3), 1684 (2003). DOI: 10.1063/1.1532939
[15] R.S. Weis, T.K. Gaylord. Appl. Phys. A, **37**, 191(1985). DOI: 10.1007/BF00614817
[16] O. Manoochehri, A. Darvazehban, M.A. Salari, S. Khaledian, D. Erricolo, B. Smida. Microwave and Optical Technology Lett., **60** (6), 1552 (2018). DOI: 10.1002/mop.31195
[17] H. Hara, J. Yoshinari, K. Sasaki, T. Kikukawa, H. Take, T. Mino, A. Shimura, Y. Takagi, H. Fukuzawa. AIP Advances, **14** (1), 015045 (2024). DOI: 10.1063/5.0171734

Translated by J.Savelyeva